Study on Vibration Isolation Performance Analysis and Optimization Design of Ship Floating Raft

Rongming Ni*, Yuefang Wang[a]

Dalian University of Technology, School of Mechanics and Aeronautics, Dalian, China
*153042142 34@163.com, ayfwang@dlut.edu.cn

Abstract. The problem of vibration and noise caused by the propulsion shaft system in modern ships has become increasingly prominent. Floating raft isolation system is an emerging technology used to reduce vibration and noise, which can effectively reduce the transmission of shaft system vibration and noise to the hull, improving the safety and comfort of ship navigation. Based on a small experimental platform for marine propulsion shaft system, this paper constructs a finite element model of the floating raft isolation system and conducts simulation analysis using ANSYS finite element software. The vibration level drop of the system is used as the evaluation index to analyse the isolation performance of the floating raft isolation system under vibration excitation. Finally, the middle raft structure in the floating raft is optimized by opening lightening holes on the rib plates of the raft structure to reduce its mass and achieve the goal of vibration reduction and noise reduction. The results show that the optimized raft structure has better isolation effect, which can effectively solve the vibration isolation problem of the propulsion shaft system and provide reference for the design of the floating raft isolation system.

Keywords: Propulsion shafting; A floating raft; Vibration and noise reduction; Optimal design

1 Introduction

With the development of the shipbuilding industry and advancements in technology, the speed and power demands of ships have been constantly increasing. However, a major issue faced by modern ships is how to effectively reduce mechanical noise, particularly the vibrations and noise[1] generated by the propulsion system. To address this problem, the adoption of a floating raft isolation system is one of the widely applied and effective approaches. Therefore, optimizing the structural design of the floating raft isolation system and enhancing its isolation performance have become important research directions in the field of ship isolation[2,3].

The floating raft isolation technology has been widely applied in the field of ship vibration reduction and noise reduction, effectively reducing the transmission of mechanical vibrations in ships, playing an important role in improving ship stealth performance and combat effectiveness[4]. Scholars at home and abroad have conducted a large amount of research on floating raft isolation systems and have achieved some results.

Among them, Zhang Heng[5] and others studied the mechanical properties and isolation performance of plate-frame floating rafts through finite element modeling，demonstrating its good performance. Guo Qi-xing[6] and others used vibration intensity and vibration level drop as indicators to compare the influence of raft frame structural parameters and shapes on isolation performance, and evaluated the isolation effect of the floating raft system. Liu Yang[7] and others improved the optimization process of the finite element method through topology optimization design, designing a floating raft isolation system with good mechanical performance. Zhang[8] et al. proposed a novel floating raft frame structure and designed floating rafts made of carbon fiber polymer materials and metal materials. They compared the frequencies and vibration characteristics of the two types of rafts through finite element modal analysis. The results showed that the raft frame made of carbon fiber polymer materials had better vibration reduction performance. Sun[9] studied the influence of the parameters of the intermediate raft frame and the elasticity of the base on the isolation performance of the floating raft. The results showed that appropriate intermediate raft frame stiffness and damping can improve the effectiveness of the floating raft isolation system. In this study, a finite element model of the propulsion shaft system and the floating raft isolation system will be established. Simulation analysis will be conducted using ANSYS Workbench, and the vibration level drop will be used to evaluate the isolation performance of the floating raft system, providing reference for practical engineering.

2 Establishment of Finite Element Model

2.1 Shafting Parameters and Modeling

To reduce computational load, a two-dimensional axisymmetric model was employed in this study for the analysis of the shaft system. The shaft system test rig consists of a propeller, stern shaft, stern bearing and pedestal, intermediate shaft, thrust shaft, thrust bearing and pedestal, sliding bearing and pedestal, and coupling, as shown in Figure 1. The finite element model considers the stiffness of each bearing, as presented in Table 1. To handle the large size of the bearing pedestals, a solid modeling approach was utilized. This approach effectively reduces the computational load while maintaining accurate analysis of the shaft system.

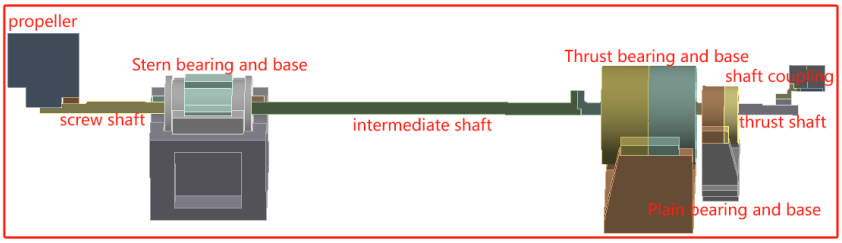

Fig. 1. Finite element model of shafting test bed.

Table 1. Individual bearing stiffness.

	Stern bearing	Thrust bearing radial
K_{xx}/(N/m)	2×10^9	2×10^7
K_{yy}(N/m)	2×10^9	2×10^7
K_{xy}(N/m)	-2×10^{10}	1.49×10^5
Kyx(N/m)	-2×10^{10}	1.49×10^5

2.2 Parameters and Modeling of Floating Raft Vibration Isolation Systems

The floating raft isolation system consists of three main components: the central raft frame, vibration isolators, and vibration equipment. The raft frame is modeled as a solid structure and consists of an upper and lower board, with dimensions of 2m×0.6m×0.01m. The central raft frame includes transverse and longitudinal rib plates, with a uniform thickness of 5mm. In the transverse direction, the raft frame has 13 rib plates, with a distance of 0.0975m between each rib plate and the ends of the raft frame, and a spacing of 0.145m between adjacent rib plates. In the longitudinal direction, the raft frame has 5 rib plates, with a distance of 0.0575m between each rib plate and the ends of the raft frame, and a spacing of 0.115m between adjacent rib plates. The initial mass of the raft frame is 222.146kg. The finite element model of the system is shown in Figure 2, and its internal structure is depicted in Figure 3.

This study utilized a total of 18 isolators as crucial components for connecting the shaft system and the floating raft. Among these, the upper isolators employed WHG-150 rubber isolators[10], with a lateral stiffness of 128N/mm, longitudinal stiffness of 260N/mm, vertical stiffness of 220N/mm, and a damping ratio of 0.07. These upper isolators were positioned between three bearing bases and the bottom plate of the raft, with four isolators at each location. The lower isolators utilized JSD-530 isolators, which are composed of a combination of metal and rubber. They had a lateral stiffness of 750N/mm, longitudinal stiffness of 1000N/mm, vertical stiffness of 750N/mm, and a damping ratio of 0.07. The isolator parameters are presented in Table 2 and 3.

Install the base to simulate the hull structure, and use SOLID185 unit to simulate the size of 2.3m×0.8m×0.03m, and do fixed constraint treatment on the bottom surface of the base. The modeling parameters of floating raft vibration isolation system are shown in Table 4 below.

Table 2. Upper vibration isolator parameter table.

	Horizontal	Longitudinal	Vertical
stiffness coefficient $\boldsymbol{k}$ (N/mm)	128	260	220
critical damping coefficient $\mathbf{C_0}$ (N·s/mm)	8	11.402	10.488
damping ratio ζ	0.07	0.07	0.07
damping coefficient $\mathbf{C}$ (N·s/mm)	2.192	0.798	0.734

Table 3. Lower vibration isolator parameter table.

	Horizontal	**Longitudinal**	**Vertical**
stiffness coefficient ***k*** (N/mm)	750	1000	750
critical damping coefficient $\mathbf{C_0}$ (N·s/mm)	31.309	36.152	31.309
damping ratio ζ	0.07	0.07	0.07
damping coefficient **C** (N·s/mm)	2.192	2.531	2.192

Table 4. Modeling parameter.

	Floating raft rack	**Base**
Size	2m×0.6m×0.07 m	2.3m×0.8m×0.03 m
Young modulus	2×10^{11} Pa	2×10^{11} Pa
Poisson's ratio	0.3	0.3
Density	7850 kg/m^3	7850 kg/m^3

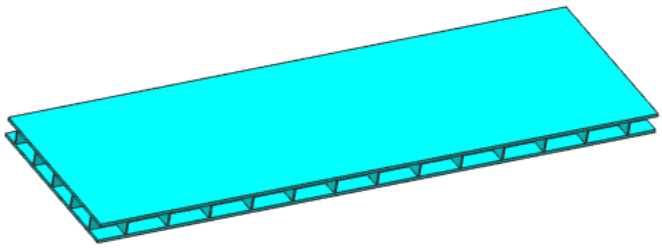

Fig. 2. Finite element model of raft.

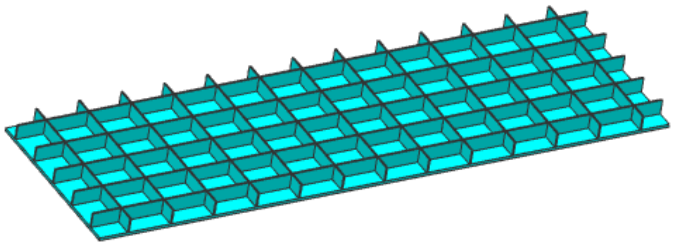

Fig. 3. Internal structure of raft.

3 Fem Simulative Analysis

The floating raft isolation system is a common vibration isolation device on ships, mainly composed of the propulsion shaft system, upper isolator, lower isolator, and intermediate raft frame. In the finite element analysis, the isolator is simulated using the COMBIN14 element. The propulsion shaft system and the base are connected to the raft frame through the upper isolator, while the raft frame is installed on the base through the lower isolator. Fixed constraints are applied to the bottom surface of the base to ensure the stability of the model. The finite element simulation model of the floating raft isolation system established using ANSYS Workbench software is shown in Figure 4.

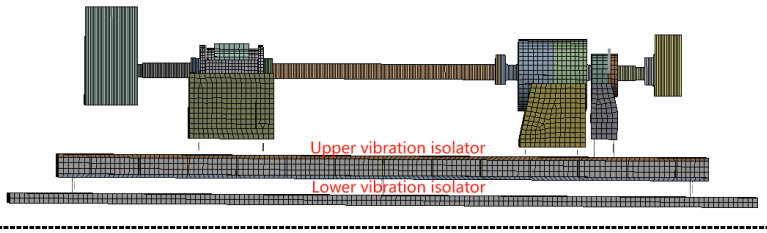

Fig. 4. Internal structure of raft.

3.1 Modal Analysis

Modal analysis is the most fundamental method in dynamic analysis and serves as the basis for other dynamic analyses. It has a wide range of applications and can assist in determining the natural frequencies and mode shapes of a structure, thereby enabling the avoidance of resonance in structural design. The natural frequency of a floating raft structure is crucial in the design of isolation systems as it reflects the inherent vibration characteristics of the raft structure. This forms the foundation for analyzing the dynamic properties of the isolation system for a floating raft.

When conducting modal analysis on the floating raft isolation system, the focus is on the influence of low-order modes on vibration characteristics[11]. Therefore, we only consider the results of the first 6 modes, excluding the first six rigid body modes, as shown in Table 5.

Table 5. The first six modes of the raft.

Order	Frequency/Hz	Modal characteristics
1	122.51	First order longitudinal bending
2	203.47	torsion
3	313.38	Second order longitudinal bending
4	402.77	Transverse bending and torsion compound
5	556.45	Third order longitudinal bending
6	595.42	transverse bending

From Table 5, it can be seen that the natural frequency of the floating raft frame is much higher than the operating frequency of the shaft system, indicating that there will be no resonance between them. Additionally, the floating raft frame possesses a certain level of rigidity, indicating a reasonable design.

A modal analysis of the entire floating raft isolation system was conducted, and the results for the first 20 modes are presented in Table 6. It can be observed from Table 6 that the floating raft isolation system exhibits several closely spaced modal frequencies, such as the 3rd and 4th natural frequencies, as well as the 8th and 9th natural frequencies. The modal shapes are depicted in Figures 5-8.

Table 6. Modal frequency value of floating raft isolation system.

Order	Frequency/Hz	Order	Frequency/Hz
1	6.909	11	35.107
2	9.6873	12	34.316
3	10.196	13	38.831
4	11.411	14	82.476
5	14.029	15	89.084
6	15.475	16	90.541
7	16.517	17	94.516
8	26.309	18	120.88
9	27.687	19	124.77
10	32.275	20	176.37

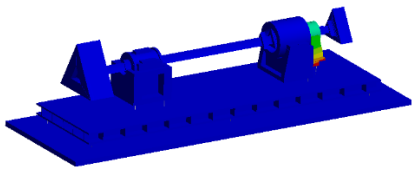

Fig. 5. The 3rd MODE (10.196Hz).

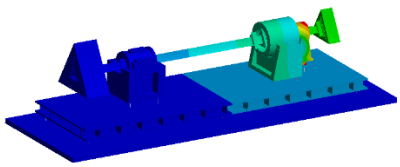

Fig. 6. The 4th MODE (11.411Hz).

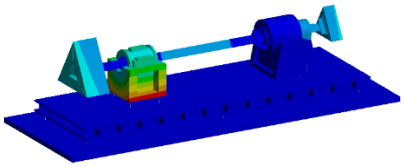

Fig. 7. The 8th MODE (26.309Hz).

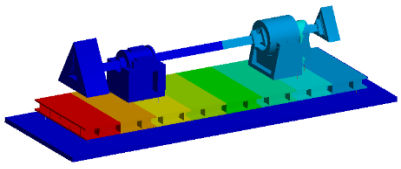

Fig. 8. The 9th MODE (27.687Hz).

3.2 Vibration Level Difference

The main methods used to evaluate the effectiveness of vibration isolation currently include force transmissibility, insertion loss, vibration intensity, and power flow. Among these methods, vibration level difference is an easily implemented approach. Depending on the measured vibration response, it can be classified into displacement level difference, velocity level difference, and acceleration level difference. Due to the common use of acceleration sensors for measuring acceleration in practical engineering, acceleration level difference is more widely applied[12].

Vibration acceleration is expressed as vibration acceleration level by level, referred to as vibration level L, and its expression is as follows:

$$L = 20log\frac{a_1}{a_0} \tag{1}$$

Where, a_1 is the acceleration of the measuring point; a_0 is the base acceleration, a_0=10^{-6} mm/s^2.

In order to reduce the measurement error, n nodes of a certain layer are usually taken to form a response node group, and it is reasonable to analyze the average vibration level of this response node group. The average value of n measuring points is taken as the measurement result, and the calculation expression of the average vibration level $\overline{L}$ is as follows:

$$\overline{L} = 10log\left(\frac{1}{n}\sum_{i=1}^{n}10^{\frac{L_i}{10}}\right) \tag{2}$$

Where, L_i is the vibration level of the i th measuring point.

The vibration level difference is obtained by taking the logarithm of the ratio between the effective value of the vibration response of the isolation device and the effective value of the corresponding base response, and then multiplying it by a constant of 20, and its expression is as follows:

$$L_D = 20log\frac{a_1}{a_0} - 20log\frac{a_2}{a_0} = L_{a_1} - L_{a_2} \tag{3}$$

Where, L_D is the vibration level drop between measured points, the unit is dB; a_1 and a_2 are the acceleration of the measuring point respectively; a_0 is the base acceleration, a_0=10^{-6} mm/s2; L_{a1} and L_{a2} are the vibration levels of the measured points respectively, the unit is dB.

When the vibration level drop L_d of the total acceleration level is taken for calculation, there are:

$$L_d = 20lg\frac{\sqrt{\left(a_{i1}^2 + a_{i2}^2 + ... + a_{in}^2\right)}}{\sqrt{\left(a_{j1}^2 + a_{j2}^2 + ... + a_{jn}^2\right)}} \tag{4}$$

3.3 Analysis of Isolation Characteristics of Floating Raft Isolation System

Using ANSYS software, a complete method is employed to analyze the harmonic response of a floating raft isolation system. The frequency range considered is from 0 to 400 Hz, with a solution interval of 200. A excitation force is applied at the center of the propeller hub, while the bottom of the base is fixed using a supported boundary condition. By outputting the calculation results, the vibration response of the floating raft isolation system under the excitation force can be obtained.

In this study, we used the vibration level difference as an indicator to evaluate the isolation effect. The vibration levels of each axis with respect to the base were calculated, and the vibration level curve and level difference curve of the bearing base were obtained using the calculation formula, as shown in Figures 9-12. From the level difference curve, it can be observed that the isolation effects of the stern bearing and the sliding bearing are similar, while the isolation effect of the thrust bearing is noticeably stronger than the former two. Overall, as shown in Table 7, the vertical vibration level drop for the stern bearing is -2.043 dB, and for the sliding bearing, it is -4.812 dB. This has not reduced vibration but rather intensified it. In contrast, the thrust bearing shows a vertical vibration level drop of 30.080 dB, indicating excellent vibration isolation at its base. In summary, the thrust bearing performs remarkably well in vibration reduction, whereas the stern and sliding bearings exhibit poorer performance.

Table 7. The calculation result of vibration level drop.

	Vertical vibration level drop total level/dB
Stern bearing	-2.043
thrust bearing	30.080
sliding bearing	-4.812
Upper vibration isolator	15.538
Lower vibration isolator	130.282

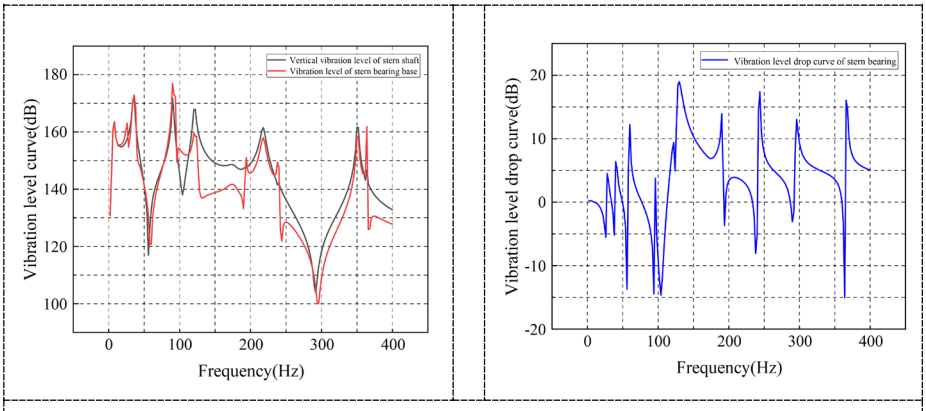

Fig. 9. (a)Vibration level curve of stern bearing;(b) Vibration level drop curve of stern bearing

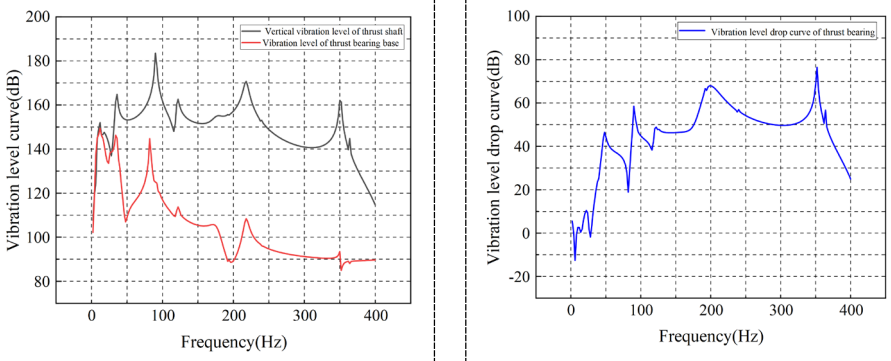

Fig. 10. (a)Vibration level curve of thrust bearing;(b) Vibration level drop curve of thrust bearing.

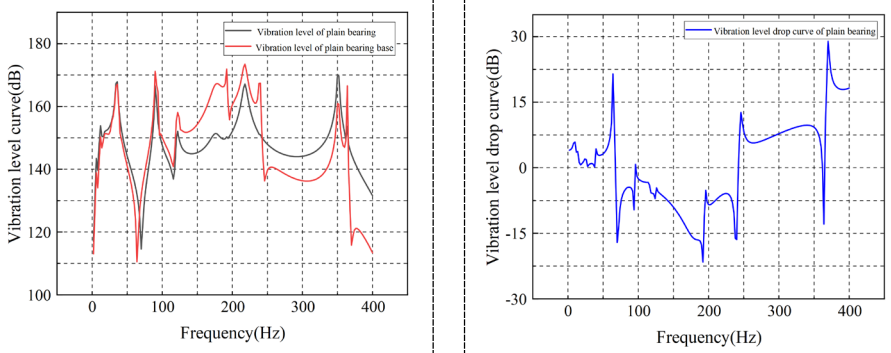

Fig. 11. (a)Vibration level curve of plain bearing;(b) Vibration level drop curve of plain bearing.

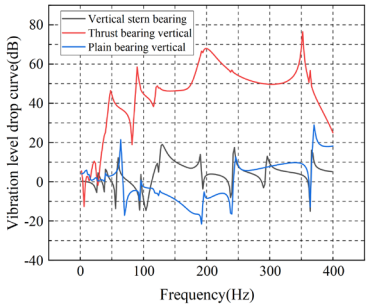

Fig. 12. Vibration level drop curve of bearing base.

Calculate the vibration level separately for each bearing pedestal and the upper plate of the raft frame. The measurement point is taken at the connection of the upper isolator. The vibration level curve and the vibration level drop curve of the upper isolator are obtained through calculation, as shown in Figure 13. From the vibration level drop curve, it can be seen that the upper isolator has good medium to high-frequency isolation performance, with a total level drop of 15.538dB. It can achieve a vibration isolation effect of 5-25dB in the low-frequency range and up to 35dB in the high-frequency range, and the isolation effect shows a significant upward trend with increasing frequency. Significant peaks and valleys appear in the vibration level drop near the positions of 27Hz, 38Hz, 83Hz, and 123Hz. Comparing with the overall natural frequencies of the floating raft isolation system, the 9th, 13th, 14th, and 19th natural frequencies are 27.687Hz, 38.381Hz, 82.476Hz, and 124.77Hz, respectively. This may be due to the resonance between the excitation force and the isolation system.

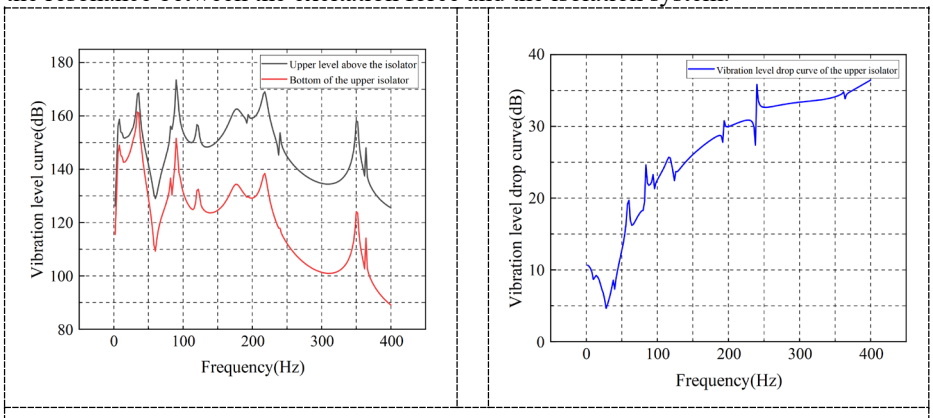

Fig. 13. (a)Vibration level curve of the upper isolator; (b) Vibration level drop curve of the upper isolator.

When measuring the vibration level of the board under the raft frame and the base separately, the connection point at the lower isolator was selected as the measurement point. By using a calculation formula, the vibration level curve and the level drop curve of the lower isolator were obtained, as shown in Figure 14. From the results of the level drop curve, it can be seen that the lower isolator has good isolation performance in the low-frequency range, with a total level drop of 130.282 dB. In the low-frequency range, it can achieve an isolation effect of 130 dB, and it can also achieve an isolation effect of 107 dB in the high-frequency range. However, as the frequency increases, it is observed that the isolation effect shows a significant decrease.

In conclusion, the raft isolation system has demonstrated good vibration isolation performance. By comparing the modal analysis results of the raft structure and the isolation system, it is observed that both exhibit similar vibration characteristics at 122.51Hz in bending and 203.47Hz in torsion. This indicates that the inherent modes of the raft structure are also present in the isolation system, highlighting the significant influence of the raft's vibration characteristics on the isolation effectiveness. Furthermore, it implies that modifying the raft structure can have a considerable impact on the

isolation performance, thus optimizing the raft structure can further enhance the isolation capability.

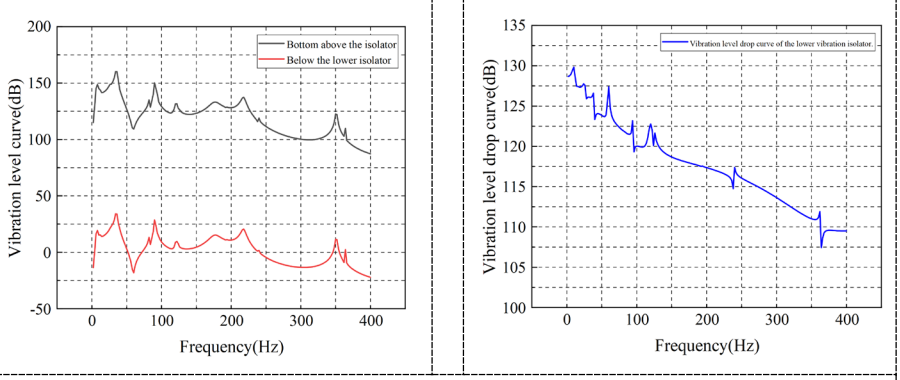

Fig. 14. (a)Vibration level curve of the lower isolator;(b) Vibration level drop curve of the lower vibration isolator.

4 Optimization of Raft Structure

In this section, the floating platform raft frame was optimized by introducing lightening holes in the transverse and longitudinal rib plates of the middle raft frame. After optimization, the weight of the floating platform raft frame was reduced by 7.4kg, reaching 214.746kg. The optimized finite element model is shown in Figure 15.

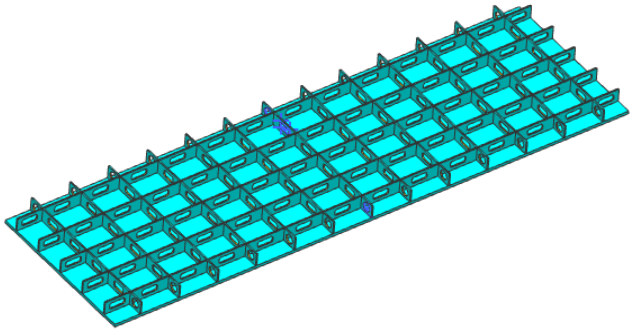

Fig. 15. Finite element model of floating raft raft frame after opening holes.

We investigated the vibration reduction performance of the floating raft system through finite element analysis. By introducing openings in the raft frame and conducting finite element analysis, we obtained the vibration level difference curves of the modified floating raft system's upper-side and lower-layer isolators, as shown in Figure 16. These curves indicate that the modified floating raft system exhibits higher

vibration level differences across the entire frequency range compared to the original model. This suggests that the vibration reduction performance of the floating raft system has been improved by modifying the rib plate structure of the raft frame. The introduction of openings has impacted the rigid and damping characteristics of the raft frame structure, thereby enhancing the isolation effectiveness of the raft body towards vibrational energy.

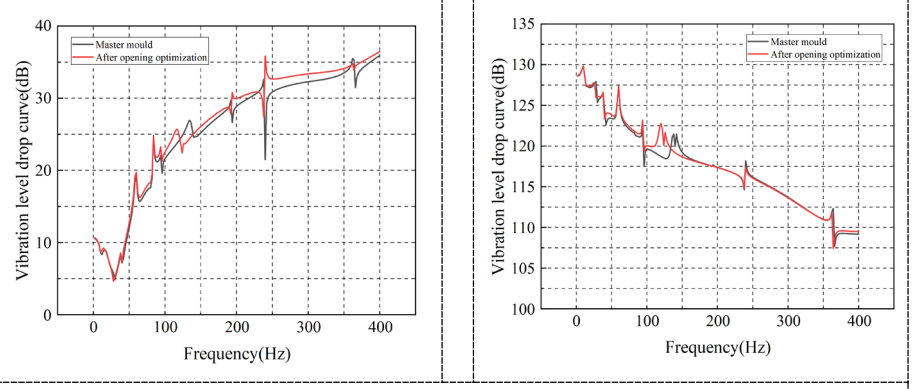

Fig. 16. (a)Vibration level drop curve of the upper isolator; (b)Vibration level drop curve of the lower vibration isolator.

5 Conclusion

This study is conducted based on the Ansys software to establish a coupled system model of propulsion shaft-raft frame-hull and evaluates the vibration isolation performance of a typical flat-plate raft frame structure. The main conclusions of the study are as follows:

1. It is found that the stiffness of the intermediate raft frame has a significant influence on the acceleration transmissibility. Reducing the stiffness of the raft body is detrimental to the effectiveness of vibration isolation. The acceleration transmissibility curve of the floating raft isolation system is solved to analyze its vibration isolation effectiveness under actual loading conditions.
2. The impact of modifying the raft frame structure through aperture openings on the transmission of vibration energy by the damping device is analyzed. The results demonstrate that opening apertures in the rib plate can effectively improve the vibration isolation performance of the device.
3. Although the optimization design in this study is based on a simple plate-type raft frame, the research methodology is applicable to the optimization design of complex floating raft isolation systems. Therefore, this study provides a foundation for further optimization design of complex floating raft isolation systems.

Acknowledgment

The authors thank the National Science and Technology Major Project (Grant 2019-IV-0019-0087) for financial support.

References

1. T. Huaicheng, Y. Yini and L. Ye. (2023) Research review on vibration reduction and isolation technology and calculation methods of Marine machinery, Applied mathematics and mechanics, vol.44, no.12, pp. 1413-1427. https://d.wanfangdata.com.cn/periodical/hjgcdxxb202104010.
2. X. Chengshi, W. Shaowei, and H. Guowen. (2022) Design and Optimization of Floating Raft Vibration Isolation Systems for Large Marine Diesel Generator Sets, Noise and Vibration Control. vol. 42, no.03, pp.25-29+35. https://lib.cqvip.com/Qikan/Article/Detail?id=7107484475&from=Qikan_Search_Index.
3. M. Siwei, Z. Baocheng, M. Cuizhen and L. Guanghua, (2024) Optimization and Vibration Reduction Effect Analysis of Double Bottom Structures, Noise and Vibration Control, vol.44, no. 01, pp.86–91, 2024. https://nvc.sjtu.edu.cn/CN/Y2024/V44/I1/86.
4. X. Mingcheng, X. Shaoyu and W. Ruhang, (2024) Performance optimization and lightweight design of floating raft vibration isolation system based on RBF-PSO algorithm, Chinese ship research. DOI: 10.19693/j.issn.1673-3185.03687.
5. Z. Heng and H. Xia-xia and S. Shi-gang, (2013) Design and study of vibration isolation characteristics of frame floating raft, master's thesis, Zhejiang University of Technology. DOI: 10.7666/d.y2142894.
6. G. Qi-xing and W. Xiaotian, (2018) The design and study of the structure type of ship flat slab floating raft, master's thesis, Harbin Engineering University. CNKI: CDMD: 2.1018.048078.
7. L. Yang and C. Guo-ping, (2016) Optimization Design of Floating Raft Isolation System Based on the Finite Element Method, master's thesis, Nanjing University of Aeronautics and Astronautics. https://xueshu.baidu.com/usercenter/paper/show?paperid=1m0h0x40ag4e0ev09f7n00809k324387.
8. Z. Jinguang, Y. Hairu, C. Guozhi and Z. Zeng, (2018) Structure and modal analysis of carbon fiber reinforced polymer raft frame, Journal of Low Frequency Noise Vibration and Active Control, vol. 37, no. 3, pp.577–589. DOI: 10.1177/1461348417725960.
9. H. Sun, (2016) Simplified performance indices and active control force of vibration isolation systems with elastic base, Shengxue Xuebao/Acta Acustica, vol.41, issue.2, pp. 227–235.
10. S. Meng, Q. Changlin and Z. Shiyang, (2023) Research on vibration isolation performance of modular floating raft system of pump equipment, Ship science and technology, vol.45, no.03, pp. 32-38. https://xueshu.baidu.com/usercenter/paper/show?paperid=1b0d0mm03d0b08808f760cy0yk343747&site=xueshu_se.
11. G. Peng, Z. Qizheng and W. Deshi, (2023) Study on low frequency vibration isolation performance of local resonant floating raft isolation system, Journal of Dynamics and Control. vol.21, no.07, pp. 59-67. https://d.wanfangdata.com.cn/periodical/dlxykzxb202307009.
12. Z. Nan, W. Yu and C. Lin, (2022) Study on vibration isolation performance of distributed acoustic black hole floating raft system, Vibration and shock.vol.41, no.13, pp.75-80. DOI: 10.13465/j.cnki.jvs.2022.13.010.